ELSEVIER

Journal of Biomechanics 37 (2004) 1439–1446

JOURNAL OF BIOMECHANICS

www.elsevier.com/locate/jbiomech
www.JBiomech.com

Short communication

# Segment-interaction analysis of the stance limb in sprint running ☆

Joseph P. Hunter[a,*], Robert N. Marshall[a,1], Peter J. McNair[b]

[a] *Department of Sport and Exercise Science, The University of Auckland, Private Bag 92019, Auckland, New Zealand*
[b] *School of Physiotherapy, Physical Rehabilitation Research Centre, Auckland University of Technology, Auckland, New Zealand*

Accepted 16 December 2003

**Abstract**

A high angular velocity of the thigh of the stance limb, generated by hip extensor musculature, is commonly thought to be a performance-determining factor in sprint running. However, the thigh segment is a component of a linked system (i.e., the lower limb), therefore, it is unlikely that the kinematics of the thigh will be due exclusively to the resultant joint moment (RJM) at the hip. The purpose of this study was to quantify, by means of segment-interaction analysis, the determinants of sagittal plane kinematics of the lower limb segments during the stance phase of sprint running. Video and ground reaction force data were collected from four male athletes performing maximal-effort sprints. The analysis revealed that during the first-third of the stance phase, a hip extension moment was the major determinant of the increasing angular velocity of the thigh. However, during the mid-third of stance, hip and knee extension moments and segment interaction effects all contributed to the thigh attaining its peak angular velocity. Extension moments at the ankle, and to a lesser extent the knee, were attributed with preventing the 'collapse' of the shank under the effects of the interactive moment due to ground reaction force. The angular acceleration of the foot was determined almost completely by the RJM at the ankle and the interactive moment due to ground reaction force. Further research is required to determine if similar results exit for a wide range of athletes and for other stages of a sprint race (e.g. early acceleration, maximal velocity, and deceleration phases).


*Keywords:* Inverse dynamics; Interactive moments; Resultant joint moments; Kinetics; Proximal-to-distal sequence

## 1. Introduction

In athletics, superior sprint running performance is often attributed, at least in part, to the athlete having powerful hip extensor musculature. It is thought that during the stance phase, the hip extensors (particularly the hamstrings and gluteus maximus muscles) are responsible for driving the stance thigh rearward, thereby producing a large horizontal ground reaction impulse to propel the athlete forward with increased velocity. Scientific support for this 'hip extensor theory' arises from associations between sprint performance and angular kinematics of the stance thigh (Kunz and Kauffman, 1981; Mann and Herman, 1985; Mann and Sprague, 1983), hip extension strength (Guskiewicz et al., 1993), and hip extensor electromyograph activity (Wiemann and Tidow, 1995).

Inverse dynamic analysis has previously been used to examine the kinetics of the lower limbs in sprinting (Johnson and Buckley, 2001; Mann and Sprague, 1980, 1983; Mann, 1981; Wood, 1987). These studies reported the resultant joint moment (RJM) acting at the proximal end of each segment. While there is nothing inherently wrong with this approach, to the unwary it might promote the notion that the proximal RJM is the only determinant of the segment's angular acceleration. However, this is only true if the segment is in total isolation from all other influences (Putnam, 1991), which in gait is very unlikely. Other possible contributors to the angular acceleration of a segment include the RJM at the distal end of the segment, and less obviously, all the other resultant joint moments of the linked system (Putnam and Dunn, 1987). The effects of these 'other resultant joint moments' are transferred among segments by resultant joint forces. Such an occurrence is called 'segment interaction.'

☆ Supplementary data associated with this article can be found, in the online version, at doi: 10.1016/j.jbiomech.2003.12.018

*Corresponding author. Fax: +64-9-373-7043.
*E-mail address:* joe.hunter@xtra.co.nz (J.P. Hunter).
[1] Current address: Faculty of Health and Sport Science, Eastern Institute of Technology, Hawkes Bay, New Zealand.

0021-9290/$ - see front matter © 2004 Elsevier Ltd. All rights reserved.
doi:10.1016/j.jbiomech.2003.12.018

**Nomenclature**

$m_f, m_s, m_t$ mass of the foot, shank, and thigh
$I_{cmf}, I_{cms}, I_{cmt}$ moment of inertia about the centre of mass of the foot, shank, and thigh
$\phi_f, \phi_s, \phi_t$ segment angles for the foot, shank, and thigh, measured at the proximal joint, counter-clockwise from right hand horizontal
$\omega_f, \omega_s, \omega_t$ angular velocities of the foot, shank, and thigh
$\alpha_f, \alpha_s, \alpha_t$ angular accelerations of the foot, shank, and thigh
$r_{af}, r_{ks}, r_{ht}$ distances from the proximal joint to the centre of mass of the foot, shank, and thigh
$l_s, l_t$ lengths of the shank and thigh segments
$GRF_X, GRF_Y$ $X$ and $Y$ components of the ground reaction force
$a_{Xh}, a_{Yh}$ $X$ and $Y$ components of the linear acceleration of the hip
$d_{Xcop}, d_{Ycop}$ $X$ and $Y$ distances from the centre of mass of the foot to the centre of pressure (i.e., $X_{cop}-X_{cmf}$ and $Y_{cop}-Y_{cmf}$, respectively, where $X_{cop}$ and $Y_{cop}$ are the $X$ and $Y$ co-ordinates of the centre-of-pressure, and $X_{cmf}$ and $Y_{cmf}$ are the $X$ and $Y$ co-ordinates of the centre of mass of the foot)
$g$ gravitational constant

*Moments acting on the foot (Eq. (1)):*
$I_{cmf}\alpha_f$ net moment
$RJM_{af}$ RJM at the ankle, acting on the foot
$IM_{f-h}$ interactive moment due to the linear acceleration of the hip $m_f r_{af}[a_{Xh}\sin(\phi_f) - a_{Yh}\cos(\phi_f)]$
$IM_{f-t}$ interactive moment due to the angular kinematics of the thigh $-m_f r_{af} l_t[\omega_t^2 \sin(\phi_f-\phi_t)+\alpha_t \cos(\phi_f-\phi_t)]$
$IM_{f-s}$ interactive moment due to the angular kinematics of the shank $-m_f r_{af} l_s[\omega_s^2 \sin(\phi_f-\phi_s)+\alpha_s \cos(\phi_f-\phi_s)]$
$IM_{f-f}$ interactive moment due to the angular kinematics of the foot $-m_f r_{af}^2 \alpha_f$
$IM_{f-g}$ interactive moment due to gravity $-m_f r_{af} g\cos(\phi_f)$
$IM_{f-GRF}$ interactive moment due to ground reaction force $-GRF_X[r_{af}\sin(\phi_f)+d_{Ycop}]+GRF_Y[r_{af}\cos(\phi_f)+d_{Xcop}]$

*Moments acting on the shank (Eq. (2)):*
$I_{cms}\alpha_s$ net moment
$RJM_{as}$ and $RJM_{ks}$ RJM at the ankle and knee, acting on the shank
$IM_{s-h}$ interactive moment due to the linear acceleration of the hip $[m_f l_s + m_s r_{ks}][a_{Xh}\sin(\phi_s) - a_{Yh}\cos(\phi_s)]$
$IM_{s-t}$ interactive moment due to the angular kinematics of the thigh $-[m_f l_s l_t + m_s r_{ks} l_t][\omega_t^2 \sin(\phi_s-\phi_t) + \alpha_t \cos(\phi_s-\phi_t)]$
$IM_{s-s}$ interactive moment due to the angular kinematics of the shank $-[m_f l_s^2 + m_s r_{ks}^2]\alpha_s$
$IM_{s-f}$ interactive moment due to the angular kinematics of the foot $m_f r_{af} l_s[\omega_f^2 \sin(\phi_f - \phi_s) - \alpha_f \cos(\phi_f - \phi_s)]$
$IM_{s-g}$ interactive moment due to gravity $-[m_f l_s + m_s r_{ks}]\, g\cos(\phi_s)$
$IM_{s-GRF}$ interactive moment due to ground reaction force $-l_s[GRF_X \sin(\phi_s) - GRF_Y \cos(\phi_s)]$

*Moments acting on the thigh (Eq. (3)):*
$I_{cmt}\alpha_t$ net moment
$RJM_{kt}$ and $RJM_{ht}$ RJM at the knee and hip, acting on the thigh
$IM_{t-h}$ interactive moment due to the linear acceleration of the hip $[m_t r_{ht} + m_s l_t + m_f l_t][a_{Xh}\sin(\phi_t) - a_{Yh}\cos(\phi_t)]$
$IM_{t-t}$ interactive moment due to the angular kinematics of the thigh $-[m_t r_{ht}^2 + m_s l_t^2 + m_f l_t^2]\,\alpha_t$
$IM_{t-s}$ interactive moment due to the angular kinematics of the shank $[m_f l_s l_t + m_s r_{ks} l_t][\omega_s^2 \sin(\phi_s-\phi_t) - \alpha_s \cos(\phi_s-\phi_t)]$
$IM_{t-f}$ interactive moment due to the angular kinematics of the foot $m_f r_{af} l_t[\omega_f^2 \sin(\phi_f-\phi_t) - \alpha_f \cos(\phi_f-\phi_t)]$
$IM_{t-g}$ interactive moment due to gravity $-[m_t r_{ht} + m_s l_t + m_f l_t]\, g\cos(\phi_t)$
$IM_{t-GRF}$ interactive moment due to ground reaction force $-l_t[GRF_X \sin(\phi_t) - GRF_Y \cos(\phi_t)]$

Segment interactions have previously been quantified in free-swinging limbs (Hoy and Zernicke, 1985, 1986; Putnam, 1983, 1991; Putnam and Dunn, 1987); however, no such analysis exists for the stance limb in sprint running. Therefore, the purpose of this paper was to quantify, using segment-interaction analysis, the causes of sagittal plane kinematics of the stance-limb segments during sprint running.

## 2. Methods

Four male track-and-field athletes took part in this study. Their personal-best times for 100 m ranged from 10.60 to 10.97 s. Mean ± SD for age, height, and body mass were 21 ± 3 yr, 1.81 ± 0.02 m, and 75.4 ± 6.0 kg, respectively. Approval to undertake the study was given by The University of Auckland Human Subjects Ethics Committee. Written informed consent was obtained from each athlete.

The athletes performed maximal-effort sprints on a synthetic track that passed through the laboratory. Three-dimensional kinematic data were obtained at a sampling rate of 240 Hz from eight *Falcon High Resolution Cameras* and *EVa 6.15* data collection system (Motion Analysis Corporation, Santa Rosa, CA, USA). The video capture volume was approximately 6.0 m long, 2.4 m high, and 2.0 m wide and was centred at 16 m from the sprint start line. Video calibration was performed at the beginning of each data collection session. A recessed force-plate (Bertec 6090s; Bertec Corporation, Columbus, OH, USA) located 16 m from the sprint start line was used to measure ground reaction force (GRF). The force plate signals were amplified (Bertec AM6-3 amplifier) and recorded in *EVa 6.15* at a sampling rate of 960 Hz. A matrix provided by the manufacturers, and checked for accuracy by the experimenters, was used for force calibration.

The testing session began with the athlete warming-up. Following this, markers were attached (see Table 1) and a static trial, in which the subject stood stationary was collected. Next, eight markers were removed (see Table 1), and after an additional warm-up, the athlete performed maximal-effort sprints, 25 m in length, from a standing start. The rest period between sprints, typically lasted about 4 min. Successful trials were those that the athlete clearly contacted the force plate without adjusting his natural running pattern. So this could occur, the sprint start line was adjusted by no more than 1 m. Four or five successful trials were collected from each athlete.

The lower limb was modelled as three segments: the foot, from the head of the second metatarsal to the ankle joint centre; the shank, from the ankle joint centre to the knee joint centre; and the thigh, from the knee joint centre to hip joint centre. Segment inertia parameters were obtained from de Leva (1996a), with the exception of the foot's centre of mass location and radius of gyration which were obtained from Winter (1990). The mass of the shoe (typically $\sim$200 g) was added to the mass of the foot.

From the static trial data, the hip joint centre was calculated using a method proposed by Bell et al. (1990), knee and ankle joint centres were calculated as halfway between the lateral and medial markers of the respective joint, and the head of the second metatarsal was calculated as the point where a line through the medial toe maker and perpendicular to the long axis of the foot, intersected with a plane containing the heel marker, forefoot marker and ankle joint centre. The position of each joint centre was measured relative to a group of three reference markers located on an adjacent segment. It was assumed that throughout the testing session the three markers within each group remained in fixed positions relative to one another. For the sprint trials, joint centres were calculated via knowledge of their relative positions.

From the collected three-dimensional data, two-dimensional sagittal plane coordinates were extracted and used for further analysis. The data were smoothed with a fourth-order, low-pass Butterworth filter (Winter, 1990). A cut-off frequency for each $X$ and $Y$ component of each joint trajectory was determined subjectively after viewing the raw and filtered acceleration data. Once decided upon, the same cut-off frequencies (ranging from 8 Hz for the hip joints to 12 Hz for the foot markers) were used for all athletes.

Table 1
Description of marker placement

| Marker | Position |
|---|---|
| Forefoot | On top of the second metatarsal, approximately 2.0 cm posterior from its head. |
| Medial toe* | On the medial side of the base of the big toe, so a line intersecting with the centroid of the marker and the head of the second metatarsal is perpendicular to the long axis of the foot. |
| Heel | On the most posterior surface of the calcaneous, approximately 2.0 cm above ground level when the subject is standing stationary. |
| Lateral ankle | On lateral malleolus, immediately superior ($\sim$5 mm) to its distal tip. |
| Medial ankle* | The distal tip of the medial malleolus. |
| Mid-shank | Approximately halfway up the most anterior surface of the shank. |
| Lateral knee | On the maximal protrusion of the lateral epicondyle, approximately at the level of the lower third of the patella, when the knee is extended. |
| Medial knee* | On the maximal protrusion of the medial epicondyle, approximately at the level of the lower third of the patella, when the knee is extended. |
| ASIS | Anterior superior iliac spine. |
| Mid-PSIS | Mid-way between the posterior superior iliac spines. |
| Greater trochanter* | The most lateral protrusion of the greater trochanter. |

All markers, except mid-PSIS, were on the left- and right-hand sides of the body. An asterisk indicates the markers that were removed after the static trial. To ensure a dislodged marker could be replaced precisely in its original location, marker positions were traced on the skin with ink. Pelvic and hip marker positions were based on the method proposed by Bell et al. (1990). Knee and ankle marker positions were based on information provided by Zatsiorsky (1998) and de Leva (1996b). Table adapted from Hunter, J, Marshall, R, and McNair, P., 2004. Interaction of step length and step rate during sprint running. Medicine and Science in Sports and Exercise, 36, 261–271. Reprinted with permission.

GRF data were filtered with a cut-off frequency of 75 Hz.

For the step from the force-plate, step length, step rate, and sprint velocity were calculated. The instant of touchdown for the first ground contact beyond the force plate (which was required to calculate step rate) was assumed to occur at the instant of peak vertical acceleration of the head of 2nd metatarsal (Hreljac and Marshall, 2000). The following variables were also calculated for the stance limb: segment and joint angular kinematics, resultant joint moments, and segment interactions. Data from the fastest three trials of each athlete were used in the calculation of group means.

The segment interaction equations differed slightly to those of Putnam (1991) and Hoy and Zernicke(1986). These differences were: (a) the inclusion of an external force acting on the distal segment (i.e., GRF); (b) the RJM acting at the distal end of each segment was maintained as a separate term; (c) the net moment for each segment was expressed as acting about the segment's centre of mass (i.e., instead of the proximal joint centre); and (d) the interactive moments combined the effects of both velocity and acceleration (i.e., they were not calculated as separate terms). The equations can be summarised as follows:

Equation for the foot:

$$I_{cmf}\alpha_f = RJM_{af} + IM_{f-h} + IM_{f-t} + IM_{f-s} + IM_{f-f} + IM_{f-g} + IM_{f-GRF}. \quad (1)$$

Equation for the shank:

$$I_{cms}\alpha_s = RJM_{as} + RJM_{ks} + IM_{s-h} + IM_{s-t} + IM_{s-s} + IM_{s-f} + IM_{s-g} + IM_{s-GRF}. \quad (2)$$

Equation for the thigh:

$$I_{cmt}\alpha_t = RJM_{kt} + RJM_{ht} + IM_{t-h} + IM_{t-t} + IM_{t-s} + IM_{t-f} + IM_{t-g} + IM_{t-GRF}. \quad (3)$$

When RJMs are calculated via standard inverse dynamic methods (e.g. Mann and Sprague, 1980; Winter, 1990) and via segment interaction equations, there is not exact agreement. This arises from calculating interactive moments from multiple velocity and acceleration terms, each affected by the inherent problems with filtering. The level of this disagreement, or error, was assessed by comparing the proximal RJM ($RJM_p$) calculated via standard methods, with the same moment calculated via segment interaction methods (i.e., $RJM_p = I_{cm}\alpha - RJM_d - IM$'s where $I_{cm}\alpha$ is the moment of inertia × angular acceleration of the segment, $RJM_d$ is the distal RJM calculated via standard methods, and IM's are the interactive moments for that segment, as listed in the Nomenclature). Following this, for one randomly chosen trial from each athlete, the error during the stance phase was quantified by 'mean error' (i.e., mean of the absolute values of the errors), and 'maximal error' (i.e., maximum of the absolute values of errors). These error measures were those associated with calculation of all interactive moments acting on a particular segment, therefore, were expressed as a percentage of the mean (over the stance phase) of the sum of absolute values of the interactive moments.

## 3. Results

The group mean ± SD for sprint velocity, step length, and step rate were 8.60 ± 0.24 m/s, 1.96 ± 0.05 m and 4.40 ± 0.15 Hz, respectively.

The mean error associated with the calculation of interactive moments did not exceed 3%; maximal error did not exceed 9%. Fig. 1 shows a typical example of resultant joint moments calculated using standard inverse dynamic methods and segment interaction methods.

Fig. 2 shows the horizontal (fore-aft) GRF and angular velocities of the hip, knee, and ankle joints of the stance limb. Each athlete used a proximal-to-distal sequence with regards to peak extension velocities of the hip, knee and ankle joints.

In Figs. 3–5 the terms 'clockwise' and 'counter-clockwise' are in reference to an athlete running from left to right. The mean curves generally represented the individual curves well, therefore, will be referred to in the following results.

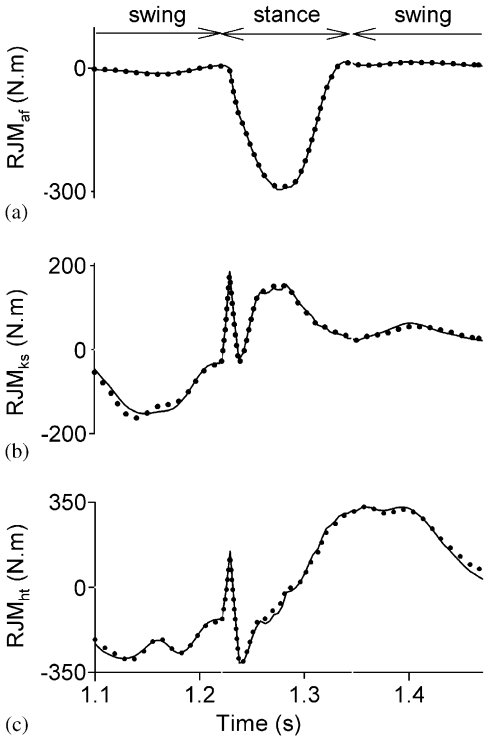


Fig. 1. Resultant joint moments at the (a) ankle, acting on the foot; (b) knee, acting on the shank; and (c) hip, acting on the thigh, calculated by standard inverse dynamic equations (solid lines) and segment interaction equations (dotted lines). These data are from a single trial.

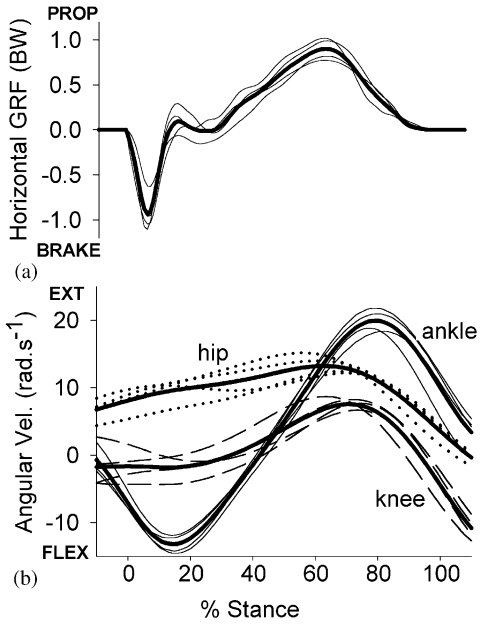


Fig. 2. (a) Horizontal (fore-aft) ground reaction force, and (b) angular velocities of the hip, knee, and ankle joints of the stance limb. Individual results are shown for each of the four athletes (thin lines) and the overall mean (heavy lines). PROP = propulsive ground reaction force, BRAKE = braking ground reaction force EXT = extension, FLEX = flexion.

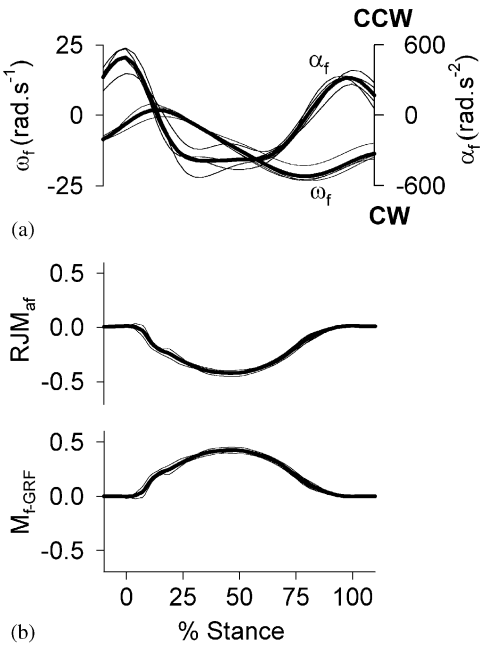


Fig. 3. (a) Angular velocity ($\omega_f$) and acceleration ($\alpha_f$) of the stance foot. CCW = counter-clockwise, CW = clockwise. (b) Two of the eight moments acting on the foot (units are $N\,m\,BW^{-1}$); the other six moments (not shown) were negligible. Just as with angular velocity and acceleration, a positive moment acts in a counter-clockwise direction, and a negative moment acts in a clockwise direction. Individual results are shown for each of the four athletes (thin lines) and the overall mean (heavy lines). The athletes ran from left to right.

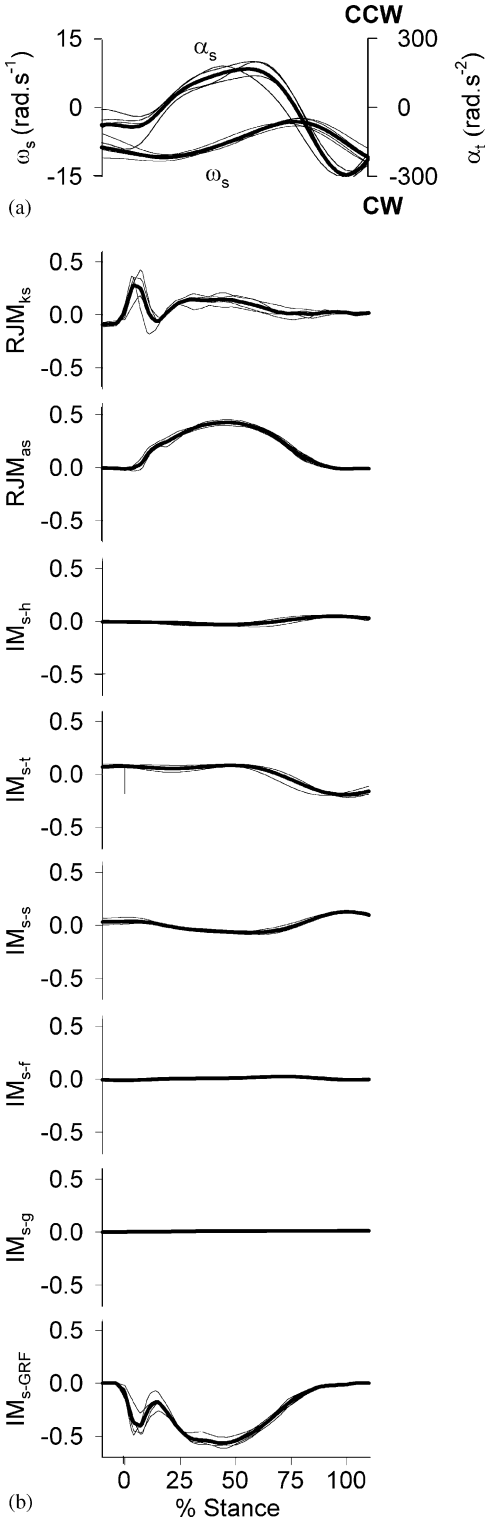


Fig. 4. (a) Angular velocity ($\omega_s$) and acceleration ($\alpha_s$) of the stance shank. CCW = counter-clockwise, CW = clockwise. (b) The eight moments acting on the shank (units are $N\,m\,BW^{-1}$). Just as with angular velocity and acceleration, a positive moment acts in a counter-clockwise direction, and a negative moment acts in a clockwise direction. Individual results are shown for each of the four athletes (thin lines) and the overall mean (heavy lines). The athletes ran from left to right.

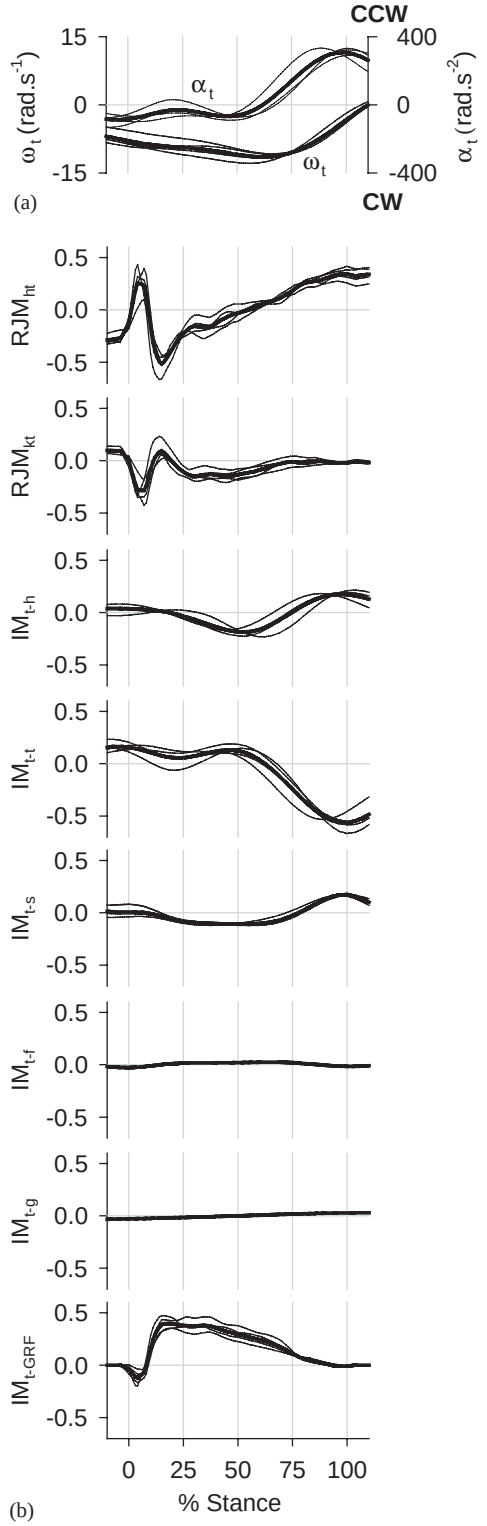


Fig. 5. (a) Angular velocity ($\omega_t$) and acceleration ($\alpha_t$) of the stance thigh. CCW = counter-clockwise, CW = clockwise. (b) The eight moments acting on the thigh (units are N m BW$^{-1}$). Just as with angular velocity and acceleration, a positive moment acts in a counter-clockwise direction, and a negative moment acts in a clockwise direction. Individual results are shown for each of the four athletes (thin lines) and the overall mean (heavy lines). The athletes ran from left to right.

During impact, the foot underwent counter-clockwise acceleration and, for a brief period, counter-clockwise velocity (Fig. 3a). Shortly after, the foot's angular acceleration changed to clockwise, and remained so until a peak clockwise velocity was obtained at about 80% stance. This clockwise acceleration during mid-stance was due to the clockwise RJM$_{af}$ dominating over the counter-clockwise IM$_{f-GRF}$ (Fig. 3b). All other moments acting on the foot were practically zero throughout the entire stance phase.

The shank underwent clockwise rotation throughout the entire stance phase, however, angular acceleration during early stance was clockwise, during mid-stance was counter-clockwise, and during late stance was clockwise again (Fig. 4a). The counter-clockwise acceleration during mid-stance was due predominantly to the two resultant joint moments, of which RJM$_{as}$ was clearly the largest. Also assisting, but to a much lesser extent, was IM$_{s-t}$ (Fig. 4b).

During approximately the first two-thirds of stance, the thigh underwent clockwise acceleration until peak clockwise velocity was obtained (at 62% stance, Fig. 5a). After the initial impact, the large clockwise RJM$_{ht}$ was the greatest contributor to this clockwise acceleration; however, it was reduced to a moderate level at about 30% stance and was reduced to zero at 54% stance (Fig. 5b). During the mid-third of stance the clockwise RJM$_{ht}$, RJM$_{kt}$, IM$_{t-h}$, and IM$_{t-s}$ all contributed to the continuing clockwise angular acceleration of the thigh. During the last third of stance the clockwise velocity of the thigh decreased (Fig. 5a) predominantly due to a large counter-clockwise RJM$_{ht}$, but also interactive moments (IM$_{t-GRF}$, IM$_{t-s}$, and IM$_{t-h}$, Fig. 5b). In contrast, IM$_{t-t}$ provided large opposition to this angular deceleration.

## 4. Discussion

Segment interaction analyses have previously been performed on open-linked systems (e.g. free-swinging limbs) often in which the goal of the task being analysed was to impart a high linear velocity to the distal end of the distal segment (e.g. Putnam, 1983, 1991; Putnam and Dunn, 1987). In contrast, we applied a segment-interaction analysis to a closed-linked system in which the distal end of the distal segment was practically 'fixed' to the ground throughout the entire period of interest. Despite these differences, a commonality between our analysis and previous open-linked analyses was the goal to determine the causes of the kinematics of the segments within the system. Such knowledge is important in sprint running because the kinematics of the stance-limb segments (particularly the thigh) are thought to play a major role in production of propulsive GRF, and in turn, sprint running performance (Mann

and Sprague, 1980, 1983; Wiemann and Tidow, 1995). Our results suggested that throughout the stance phase, angular acceleration of the foot and shank were determined predominantly by resultant joint moments and interactive moments due to GRF. However, angular acceleration of the thigh was influenced by at least six moments (two resultant joint moments and at least four interactive moments).

The calculated resultant joint moments acting at the proximal end of the foot, shank, and thigh (see Figs. 3–5) were similar in magnitude and pattern to previous results for sprinting (e.g. Johnson and Buckley, 2001). To our knowledge, there are no previous reports of interactive moments of the *stance* limb in running.

Eqs. (1)–(3) presented in the Section 2, show a condensed form of the segment interaction equations used. On the left side of each equation is the net moment, and on the right are the resultant joint and interactive moments. These equations illustrate that a segment's angular acceleration is determined by the sum effect of all the moments on the right-hand side of the equation. For the purpose of this paper, we defined interactive moments as: moments caused by components of joint forces, where the components can be gravity-, motion-, or GRF-dependent. (In this definition, the GRF acting directly on the foot was considered to be a 'joint' force with just a single component.) Note, however, that the angular position of the segment on which the moment acts, also influences the resulting interactive moment.

In-depth description and interpretation of interactive moments are provided elsewhere (Putnam, 1991, 1993), so will not be repeated here. However, the interactive moments due to GRF are a new concept, therefore, require interpretation. $IM_{f-GRF}$, $IM_{s-GRF}$, and $IM_{t-GRF}$ are the moments that would be applied by the GRF components of the joint forces acting on the foot, shank and thigh, respectively, if the system was in a condition of static equilibrium and not under the influence of gravity. The results in Figs. 3–5 show that the interactive moments due to GRF were relatively large and generally opposed the action of the resultant joint moments acting on the segment. The main exception to this was for the thigh, late in the stance phase.

The validity of the calculated moments depended on a number of factors. When compared to standard inverse dynamic methods, the level of error introduced by using multiple velocity and acceleration terms to calculate interactive moments was found to be acceptable. However, the level of error introduced by use of a simple three-segment model of the lower limb, including the foot as a single rigid segment, was unclear. Furthermore, some error due to inaccuracies in joint centre location was probable. For example, relatively small mislocations of the hip have been shown to have large effects on the magnitude and timing of the hip RJM (Stagni et al., 2000). To calculate hip joint centre location we used a method suggested by Bell et al. (1990); however, a functional method may have provided greater accuracy (Leardini et al., 1999). Consequently, until further segment interaction analyses are performed on more athletes, using a more intricate model and highly accurate joint centre locations, the kinetics shown in Figs. 3–5 should be viewed as a guide only.

The interest regarding the determinants of thigh angular kinematics, originated from what we have termed "the hip extensor theory." This popular theory (Mann and Sprague, 1980, 1983; Wiemann and Tidow, 1995) is based on the premise that the hip extensors are the major determinant of stance-thigh angular acceleration, and that a high angular velocity of the thigh contributes to production of propulsive GRF. For the four athletes in this study, the $RJM_{ht}$ was the major determinant of the clockwise acceleration of the thigh during the first third of stance. However, $RJM_{ht}$ was reduced by more than half, at about 30% through stance. Up until this point, only relatively small propulsive GRF had been produced (see Fig. 1). Conversely, during the mid-third of stance, when propulsive GRF rapidly increased, $RJM_{ht}$, $RJM_{kt}$ and interactive moments ($IM_{t-h}$ and $IM_{t-s}$) all contributed to the continuing clockwise acceleration of the thigh, and the attainment of peak clockwise velocity approximately two-thirds through stance. Therefore, while the $RJM_{ht}$ was clearly a major determinant of thigh angular acceleration during stance, the hip extensor theory failed to predict the contribution of the $RJM_{kt}$ and interactive moments.

During the final third of stance, the large counter-clockwise $RJM_{ht}$ and the continuing clockwise velocity of the thigh indicated that the hip flexors acted eccentrically to decelerate the thigh, supposedly in preparation for the upcoming swing phase. Providing large opposition to the angular deceleration of the thigh was $IM_{t-t}$ (Fig. 3b). This interactive moment should not be interpreted as the thigh directly influencing its own motion, rather, it quantifies part of the inertial load experienced by the segment (Putnam, 1991, 1993).

In contrast to the thigh, the angular acceleration of the shank and foot segments were determined almost entirely by resultant joint moments and the interaction moments due to GRF. In the case of the shank, the $RJM_{ks}$, and in particular the $RJM_{as}$, opposed the counter-clockwise $IM_{s-GRF}$, and can be viewed as preventing the 'collapse' of the shank under the effect of $IM_{s-GRF}$. The RJM at the knee has previously been highlighted as assisting in maintaining the height of the centre of mass throughout stance (Johnson and Buckley, 2001). We suggest that the RJM at the ankle has a similar role, due to its 'supporting' effect on the shank.

Up to this point, we have considered the resulting kinematics of the foot, shank, and thigh segments, separately. However, joint kinematics also revealed some interesting patterns that occurred within the stance limb. Our results agreed with reports of a proximal-to-distal sequence during the stance phase (Johnson and Buckley, 2001), and we noted that a large propulsive GRF was produced at approximately the same time as peak hip and knee extension velocities. The second part of the hip extensor theory (that we did not assess) states that a high angular velocity of the thigh is largely responsible for production of favourable GRF. Further research is required to assess the contribution of the stance-limb kinematics to production of GRF, and to assess the role of the proximal-to-distal sequence used.

Finally, although the results of the four athletes in this study were similar, the results may not necessarily be representative of other athletes and of other phases of a sprint (e.g. maximal velocity and deceleration phases). Further research is required to assess the generalisability of the results.

## Acknowledgements

Thanks to the late James G. Hay for his expert advice and encouragement. His presence is sorely missed. Thanks also to Rene Ferdinands for assisting with data collection.

## References

Bell, A.L., Pedersen, D.R., Brand, R.A., 1990. A comparison of the accuracy of several hip center location prediction methods. Journal of Biomechanics 23, 617–621.

de Leva, P., 1996a. Adjustments to Zatsiorsky–Seluyanov's segment inertia parameters. Journal of Biomechanics 29, 1223–1230.

de Leva, P., 1996b. Joint center longitudinal positions computed from a selected subset of Chandler's data. Journal of Biomechanics 29, 1231–1233.

Guskiewicz, K., Lephart, S., Burkholder, R., 1993. The relationship between sprint speed and hip flexion/extension strength in collegiate athletes. Isokinetics and Exercise Science 3, 111–116.

Hoy, M.G., Zernicke, R.F., 1985. Modulation of limb dynamics in the swing phase of locomotion. Journal of Biomechanics 18, 49–60.

Hoy, M.G., Zernicke, R.F., 1986. The role of intersegmental dynamics during rapid limb oscillations. Journal of Biomechanics 19, 867–877.

Hreljac, A., Marshall, R., 2000. Algorithms to determine event timing during normal walking using kinematic data. Journal of Biomechanics 33, 783–786.

Johnson, M.D., Buckley, J.G., 2001. Muscle power patterns in the mid-acceleration phase of sprinting. Journal of Sports Sciences 19, 263–272.

Kunz, H., Kauffman, D.A., 1981. Biomechanical analysis of sprinting: decathletes versus champions. British Journal of Sports Medicine 15, 177–181.

Leardini, A., Cappozzo, A., Catani, F., Toksvig-Larsen, S., Pettitto, A., Sforza, V., Cassanelli, G., Giannini, S., 1999. Validation of a functional method for the estimation of hip joint centre location. Journal of Biomechanics 32, 99–103.

Mann, R.V., 1981. A kinetic analysis of sprinting. Medicine and Science in Sports and Exercise 13, 325–328.

Mann, R., Sprague, P., 1980. A kinetic analysis of the ground leg during sprint running. Research Quarterly for Exercise and Sport 51, 334–348.

Mann, R., Sprague, P., 1983. Kinetics of sprinting. Track and Field Quarterly Review 83, 4–9.

Mann, R., Herman, J., 1985. Kinematic analysis of Olympic sprint performance: men's 200 m. International Journal of Sport Biomechanics 1, 151–162.

Putnam, C.A., 1983. Interaction between segments during a kicking motion. In: Matsui, H., Kobayashi, K. (Eds.), Biomechanics VIII-B. Human Kinetics, Champaign, IL, pp. 688–694.

Putnam, C.A., 1991. A segment interaction analysis of proximal-to-distal sequential segment motion patterns. Medicine and Science in Sports and Exercise 23, 130–144.

Putnam, C.A., 1993. Sequential motions of body segments in striking and throwing skills: descriptions and explanations. Journal of Biomechanics 26, 125–135.

Putnam, C.A., Dunn, E.G., 1987. Performance variations in rapid swinging motions: effects on segment interaction and resultant joint moments. In: Jonsson, B. (Ed.), Biomechanics X-B. Human Kinetics, Champaign, IL, pp. 661–665.

Stagni, R., Leardini, A., Cappozzo, A., Benedetti, M., Capello, A., 2000. Effects of hip joint centre mislocation on gait analysis results. Journal of Biomechanics 33, 1479–1487.

Wiemann, K., Tidow, G., 1995. Relative activity of hip and knee extensors in sprinting - implications for training. New Studies in Athletics 10, 29–49.

Winter, D.A., 1990. Biomechanics and Motor Control of Human Movement. Wiley, New York, pp. 11–102.

Wood, G., 1987. Biomechanical limitations to sprint running. In: van Gheluwe, B., Atha, J. (Eds.), Medicine and Sport Science, Current Research in Sports Biomechanics, Vol. 25. Karger, Basel, New York, pp. 58–71.

Zatsiorsky, V., 1998. Kinematics of human motion. Human Kinetics, Champaign, IL, pp. 284–291.